Supplemental Figure Legends:

Supplemental Figure 1 - TFEB is activated during senescence. (A) Senescence-associated β-galactosidase (SA-β-gal) staining of BEAS-2B cells on Day 0 (untreated) and Day 6 after senescence induction with either 100 nM doxorubicin, 5 μM bleomycin, or 500 μM H_2O_2. Scale bar, 32 μm. Images are representative of n = 3 independent experiments. (B) Quantification of SA-β-gal-positive cells. Data are mean ± SD from three independent experiments; statistical significance was determined by one-way ANOVA followed by Dunnett's multiple comparisons test against untreated controls. (C) SASP factor expression in control and senescent BEAS-2B cells. Bar graphs show fold change (mean ± SD) relative to untreated controls, statistical significance was determined by one-way ANOVA followed by Dunnett's multiple comparisons test against untreated controls. (D) Imaging of EdU incorporation of BEAS-2B cells after the indicated treatments. Scale bar, 10 μm. Images are representative of n = 3 independent experiments. (E) Quantification of EdU-positive cells. Data are mean ± SD from three independent experiments; statistical significance was determined by one-way ANOVA followed by Dunnett's multiple comparisons test against untreated controls. (F) Fluorescence imaging of BEAS-2B cells expressing TFEB-EGFP showing TFEB localization on Day 0 (untreated) and Day 3 after senescence induction with either 5 μM bleomycin or 500 μM H_2O_2. Scale bar, 32 μm. (G) Corresponding fluorescence imaging of ATG16L1-KO BEAS-2B cells expressing TFEB-EGFP under the same treatments. Scale bar, 32 μm. Images in (F) and (G) are representative of n = 3 independent experiments. (H) Quantification of cells with nuclear TFEB. Data are mean ± SD from three independent experiments (≥ 30 cells per replicate); statistical significance was determined by one-way ANOVA followed by Dunnett's multiple comparisons test against untreated controls.

Supplemental Figure 2 - Endogenous TFEB recapitulates CASM-dependent nuclear translocation during senescence and CASM regulates entry into senescence. (A)

Quantification of immunofluorescence staining of endogenous nuclear TFEB in wild-type, ATG16L1-, ATG12-, and ATG5-KO BEAS-2B cells on Day 0 (untreated) and Day 3 after senescence induction with 100 nM doxorubicin. Data are mean ± SD from three independent experiments (≥ 30 cells per replicate); statistical significance was determined by one-way ANOVA followed by Dunnett's multiple comparisons test against wild-type. (B) Quantification of immunofluorescence staining of endogenous TFEB in wild-type, ATG16L1-KO, ATG16L1-KO reconstituted with ATG16L1^{WT}, and ATG16L1-KO reconstituted with the CASM-defective ATG16L1^{F467A} BEAS-2B cells on Day 0 (untreated) and Day 3 after senescence induction with 100 nM doxorubicin. Data are mean ± SD from four independent experiments (≥ 30 cells per replicate); statistical significance was determined by one-way ANOVA followed by Šídák's multiple comparisons test on the pre-specified comparisons of interest. (C) Quantification of SA-β-gal-positive cells in a range of CASM-proficient and CASM-deficient cells before and after senescence induction. Data are mean ± SD from three independent experiments; statistical significance was determined by one-way ANOVA followed by Dunnett's multiple comparisons test against wild-type.

Supplemental Figure 3 - Expression of the bacterial effector protein SopF inhibits CASM. (A) Immunoblot analysis of V5-SopF and p62 in wild-type and V5-SopF-expressing BEAS-2B cells. (B) Immunoblot analysis of control or senescent (Day 3 after senescence induction) BEAS-2B cells expressing SopF and lysosomal TMEM192 3xHA. Levels of LC3 (LC3-II) on lysosomes purified via LysoIP using the HA epitope are shown. Whole-cell β-actin served as lysate loading control. Blots are representative of n = 3 independent experiments.

Supplemental Figure 4 - Inhibiting macroautophagy does not modulate TFEB activation. (A) Immunoblot analysis of ATG13 and p62 in wild-type and ATG13-KO cells. β-actin served as lysate loading control. (B) Immunoblot analysis of control or senescent

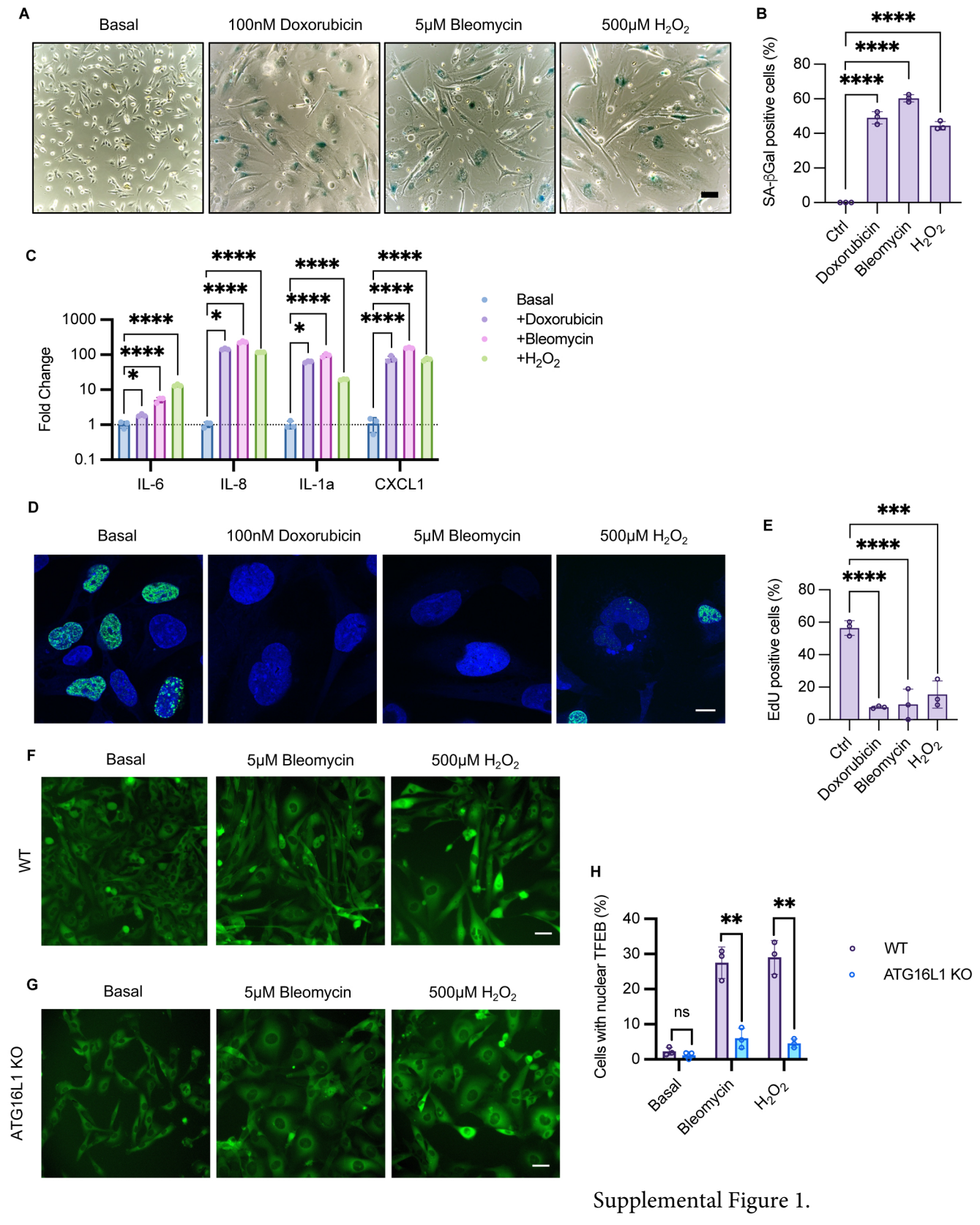
(Day 3 after senescence induction) ATG13-KO BEAS-2B cells expressing lysosomal TMEM192 3xHA. Levels of LC3 (LC3-II) on lysosomes purified via LysoIP using the HA epitope were assessed. Whole-cell β-actin served as lysate loading control. Blots are representative of n = 3 independent experiments. (C) Fluorescence imaging and (D) quantification of ATG13-KO BEAS-2B cells expressing TFEB-EGFP on Day 0 (untreated) and Day 3 after senescence induction with 100 nM doxorubicin. Scale bar, 32 μm. Images in (C) are representative of n = 3 independent experiments. In (D), data are mean ± SD from three independent experiments (≥ 30 cells per replicate); statistical significance was determined by a two-tailed unpaired t-test with Welch's correction.

Supplemental Figure 5 - Caspase-3/7 activity demonstrates CASM-dependent regulation of senescence-associated cell death. Caspase-3/7 activity (luminescence, relative light units [RLU]) in wild-type, ATG16L1-, ATG12-, and ATG5-KO BEAS-2B cells, and in ATG16L1-KO cells reconstituted with ATG16L1^{WT} or the CASM-defective ATG16L1^{F467A}, before and 3 days after senescence induction with 100 nM doxorubicin. Data are mean ± SD; statistical significance was determined by one-way ANOVA followed by Šídák's multiple comparisons test on the pre-specified comparisons of interest.

Supplemental Figure 6 - CASM is required for TFEB nuclear translocation in senescent BJ fibroblasts. (A) Fluorescence imaging of wild-type and ATG16L1-KO BJ cells expressing TFEB-EGFP showing TFEB localization on Day 0 (untreated) and Day 3 after senescence induction with 5 μM bleomycin. Boxed regions are shown at higher magnification in the right-hand panels; arrows indicate nuclear TFEB. Scale bars, 32 μm. Images are representative of n = 4 independent experiments. (B) Quantification of WT and ATG16L1-deficient BJ fibroblasts with nuclear TFEB before and after senescence induction. Data are mean ± SD from three independent experiments (≥ 30 cells per replicate); statistical significance was determined by a two-tailed unpaired t-test with Welch's correction.

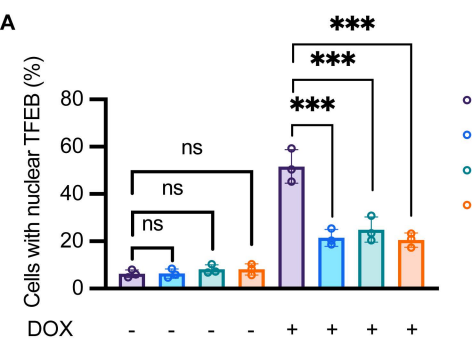
Supplemental Figure 7 - Constitutively active TFEB^{S142A} restores viability and senescence phenotypes in CASM-deficient cells. (A) Caspase-3/7 activity in wild-type, ATG16L1-KO, and ATG16L1-KO cells expressing TFEB^{S142A} before and 3 days after senescence induction with 100 nM doxorubicin. Data are mean ± SD; statistical significance was determined by one-way ANOVA followed by Dunnett's multiple comparisons test against wild-type. (B) Cell counts of wild-type, ATG16L1-KO, and ATG16L1-KO cells expressing TFEB^{S142A}. Cells were seeded at the same density on Day 0 and counted on Day 6 after senescence induction. Data are mean ± SD of three independent experiments; statistical significance was determined by one-way ANOVA followed by Dunnett's multiple comparisons test against wild-type. (C) Quantification of SA-β-gal-positive cells in wild-type, ATG16L1-KO, and ATG16L1-KO cells expressing TFEB^{S142A} on Day 0 and Day 6 after doxorubicin treatment. Data are mean ± SD of four independent experiments; statistical significance was determined by one-way ANOVA followed by Dunnett's multiple comparisons test against wild-type.

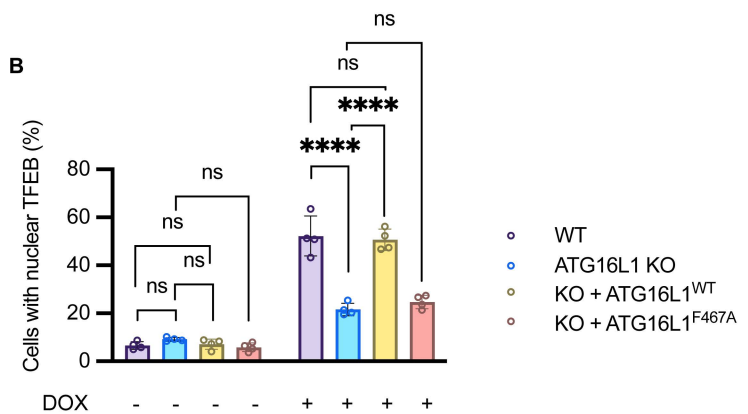
Supplemental Figure 8 - TFEB^{S142A} restores lysosomal content and viability in CASM-deficient cells after bleomycin-induced senescence. (A) Immunoblot analysis of LAMP1, cathepsin B, and β-galactosidase as markers of lysosomal content in wild-type, ATG16L1-KO, and ATG16L1-KO cells expressing TFEB^{S142A}, before and 3 days after senescence induction with bleomycin. β-actin served as lysate loading control. (B) Quantification of cell viability in wild-type, ATG16L1-KO, and ATG16L1-KO cells expressing TFEB^{S142A}, before and 3 days after senescence induction with bleomycin. Data are mean ± SD of three independent experiments; statistical significance was determined by one-way ANOVA followed by Šídák's multiple comparisons test on the pre-specified comparisons of interest.

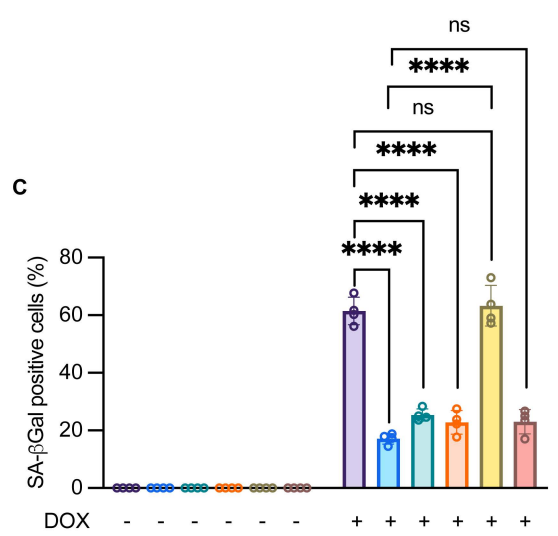


Supplemental Figure 1.

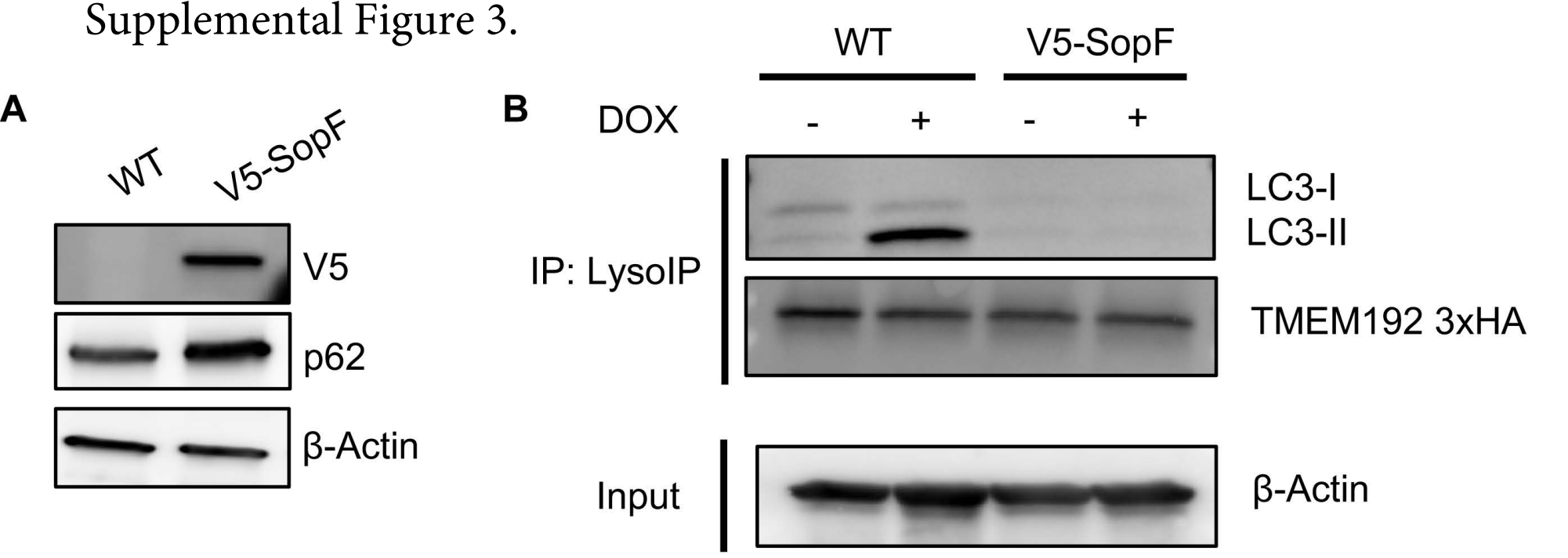
Supplemental Figure 2.

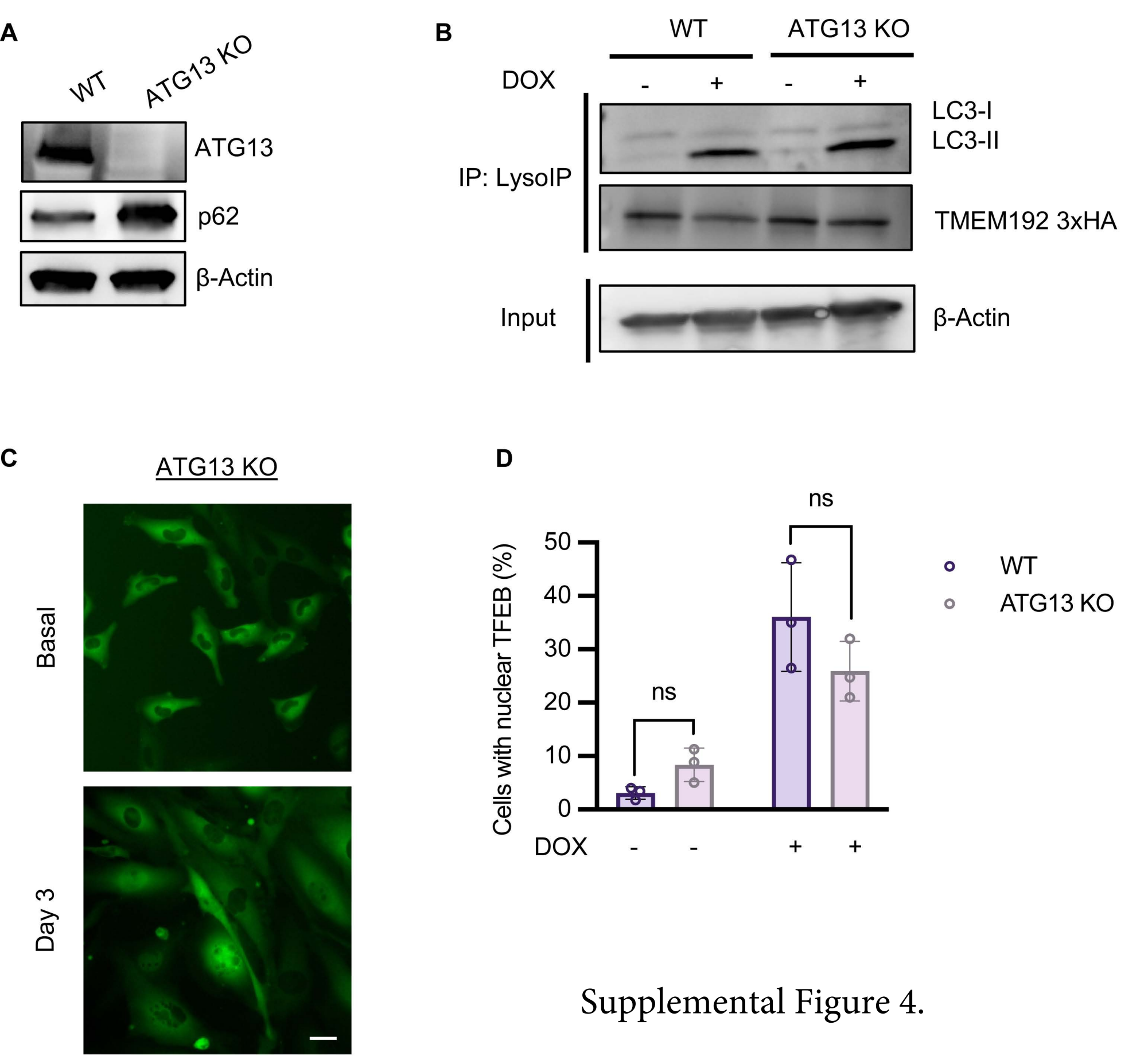






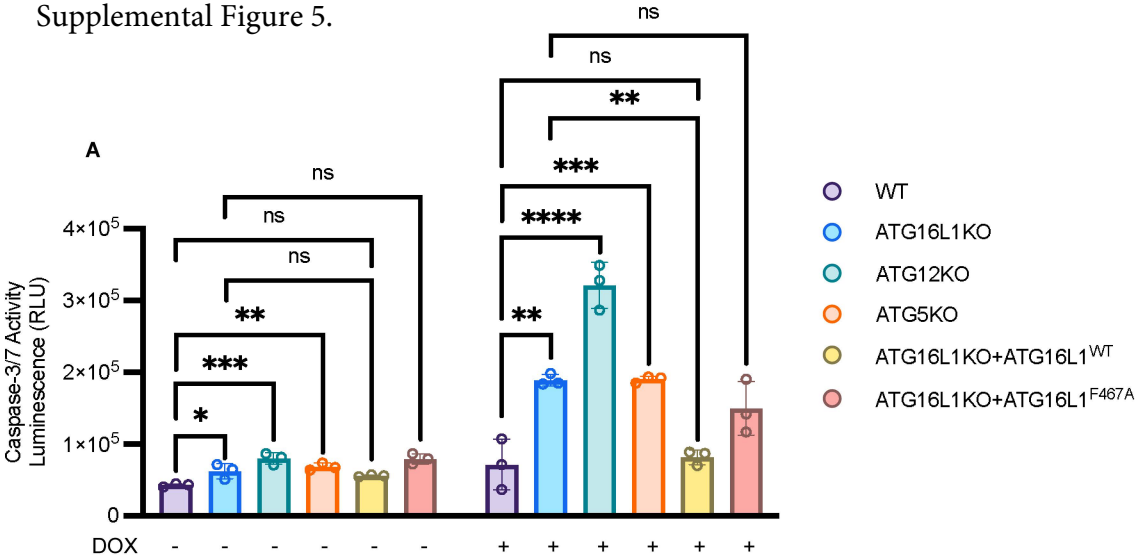
Supplemental Figure 3.



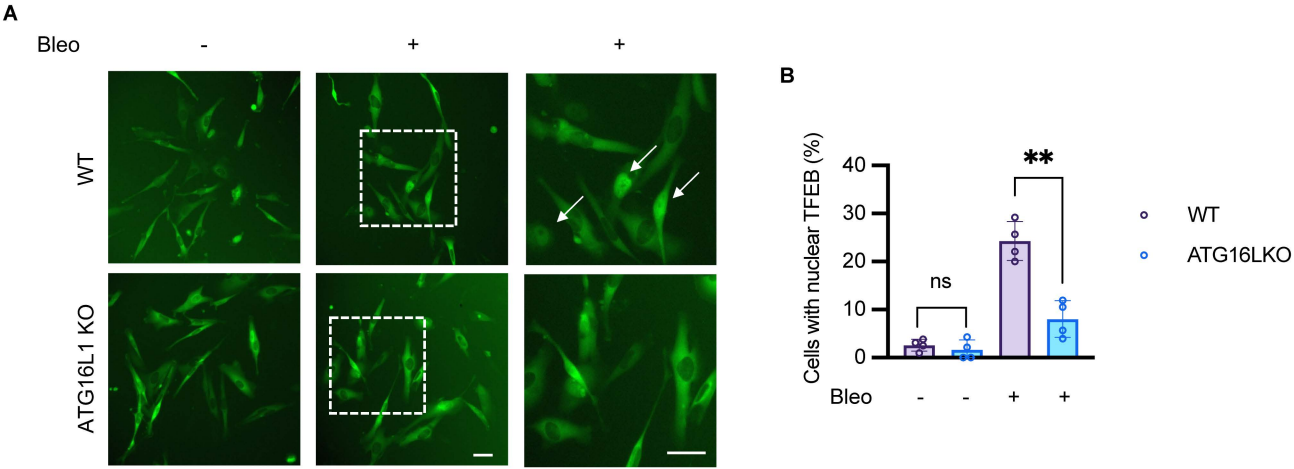


Supplemental Figure 4.

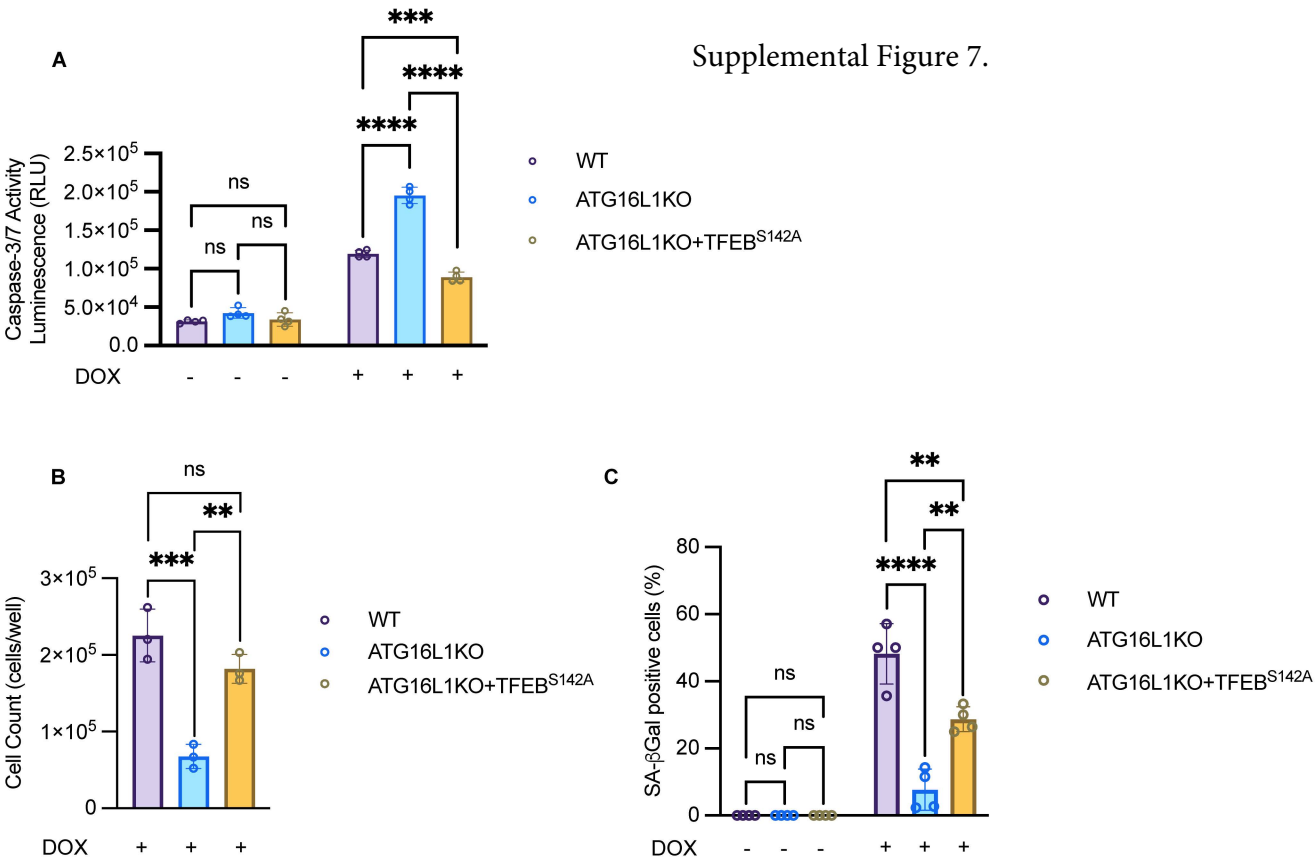
Supplemental Figure 5.



Supplemental Figure 6.



Supplemental Figure 7.



Supplemental Figure 8.

